JOURNAL OF MAGNETIC RESONANCE **130,** 300–304 (1998)
ARTICLE NO. MN971319

Improved Resolution and Signal-to-Noise Ratio in MRI via Enhanced Signal Digitization

Mark A. Elliott, Erik K. Insko, Robert L. Greenman, and John S. Leigh

Department of Radiology, University of Pennsylvania, Philadelphia, Pennsylvania 19104-6100

Received June 5, 1997; revised September 24, 1997

The high frequency *k*-space data in magnetic resonance imaging is often poorly reproduced due to the finite dynamic range of an analog-to-digital converter. The magnitude of this digitization error can equal and even exceed the magnitude of the thermal noise. Under such conditions, attempts to increase image signal-to-noise ratio via signal averaging meet with diminishing success. Because the relative size of the digitization error increases at higher spatial frequencies, a reduction in image resolution is incurred as well. By adjusting the level of the analog signal sampled by the analog-to-digital converter during the course of an imaging experiment, the magnitude of the digitization artifact can be greatly reduced. The results of simulations and imaging experiments are presented which demonstrate that this strategy improves both the signal-to-noise ratio and resolution of magnetic resonance images.

Key Words: **MRI; dynamic range; digitization noise.**

INTRODUCTION

The vast majority of magnetic resonance imaging (MRI) methods obtain spatial information by encoding the Fourier transform of an object into the NMR signal. In general, the acquired *k*-space signal has a sinc-like profile which decreases in magnitude as higher spatial frequencies are encoded. Consequently, the dynamic range of the signal increases as spatial resolution is increased. Unless care is taken to accurately reproduce the large dynamic range of high resolution MRI signals, distortion in the reconstructed image will occur.

Fourier-encoded MRI suffers from the fact that the dynamic range of the *k*-space signal is typically much greater than the dynamic range in the resulting image. Improvements in coil design and imaging at higher magnetic field strengths have increased the signal-to-noise ratio (SNR), and thereby increased the obtainable dynamic range. When the resolution of the digitizer used to capture the data is exceeded by the SNR, it becomes a limiting factor in the quality of the images produced.

Modern spectrometers typically operate with 16-bit analog-to-digital (ADC) converters. This sets the discernible dynamic range of the signal at 65536-to-1. Even at standard clinical field strengths of 1.5 T, 3D proton MRI of large volumes can have *k*-space signal-to-noise ratios which exceed this limit. For example, a $256 \times 128 \times 32$ image with an average SNR in each voxel of 100-to-1 will have an observable dynamic range in *k*-space of approximately 10^5-to-1. Under such conditions, the noise amplitude is, on average, less than 1 bit. The effective SNR is now set by the resolution of the ADC, and attempts to increase the SNR through signal averaging will yield limited results.

The limitation on image quality imposed by the resolving power of the ADC was first recognized by Maudsley (*1*) and Wedeen *et al.* (*2*), who proposed to reduce the dynamic range of the *k*-space signal by phase-scrambling with RF pulses and nonlinear gradients, respectively. Modifications of the technique have been applied using quadratic gradients in the presence of an RF pulse (*3, 4*). These methods effectively reduce the maximum amplitude of the signal, allowing the ADC to more accurately digitize the low amplitude components. The result is a measurement of the *k*-space signal with greater precision than normally afforded by the ADC. While successful to a degree, these methods are limited by the fact that the spins across each voxel are now excited with differing phase. The resulting phase dispersion produces a reduced signal intensity in the image (*5*), and consequently limits the amount by which the dynamic range of the signal can be reduced. Other approaches designed to reduce the dynamic range of MRI data include nonlinear amplitude compression (*6*) and estimation of the low spatial frequency components of *k*-space (*7*).

In this paper we demonstrate through the results of experiment and computer simulation an alternative solution to the problem of ADC-limited dynamic range which improves both the SNR and the resolution of magnetic resonance images.

THEORY

Digitization by an ADC causes a continuously valued analog signal to be approximated by a sequence of numbers with discrete values. The effect is an imperfect representation of

1090-7807/98 $25.00

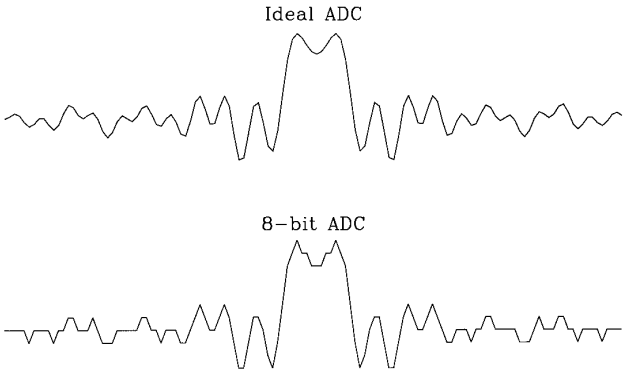

FIG. 1. Simulated *k*-space signal digitized by an essentially perfect (32-bit) ADC, and by an 8-bit ADC. The discrete data values imposed by the 8-bit ADC are clearly evident.

the original signal. Increasing the number of bits in the ADC is analogous to decreasing the step size between consecutive discrete sample values. Figure 1 depicts a simulated *k*-space signal digitized by an essentially infinite resolution (i.e., 32-bit) ADC, and by an 8-bit ADC. The discretization of low amplitude data points is clearly evident for the 8-bit ADC.

Consider an NMR signal sampled at times t_i coming from an ADC as having the form

$$f(t_i) = s(t_i) + n(t_i) + d(t_i), \qquad [1]$$

where s is the noiseless analog *k*-space signal, n is the noise due to coil and spectrometer sources, and d is the result of the discrete output of the otherwise perfect ADC. The term d is a pseudo-random function having uniform distribution with a width of one bit of the ADC's full scale. Upon discrete Fourier transformation (DFT), the signal becomes

$$f(\omega_i) = s(\omega_i) + n(\omega_i) + d(\omega_i), \qquad [2]$$

where ω_i are the frequencies at which the DFT is evaluated. As can be seen in Fig. 2, the digitization term $d(\omega)$ now appears as digitization noise (*8*) whose amplitude is frequency, and therefore spatially, dependent. It is evident that the digitization error is greatest at points where the object, $s(\omega)$, contains sharp edges. This is due to the fact that the higher frequency components of *k*-space tend to have lower amplitude, and are therefore poorly approximated by the ADC. In the case where the noise term in Eq. [1] is consistently less than the digitization term (i.e., less than one bit), the SNR of the signal is determined by the number of bits in the ADC. Moreover, the reconstructed image will have reduced resolution due to the poor reproduction of its sharp edges.

An obvious solution to the problem is to use an ADC with more digitizing bits. In practice, MRI spectrometers utilize the highest bit-level ADCs available which can operate at the sampling rates required by imaging experiments. To achieve the best digital resolution of the data, the analog signal is amplified such that the maximum signal amplitude is converted to the largest output value of the ADC. The level of signal amplification is generally fixed for the duration of the image acquisition. Most imaging sequences acquire one row of *k*-space at a time, with a TE or TR time between separate phase encodings ranging from tens of milliseconds to seconds. This time interval between acquisition windows is sufficiently long to allow setting of a new level of analog signal amplification. In many receivers, control of the signal level fed to the ADC can be changed in a matter of microseconds. In this paper, we have adjusted the receiver amplification such that the peak signal of each row of *k*-space fills the ADC. This effectively increases the dynamic range of the ADC such that it no longer limits the intrinsic SNR of the experiment. The result is an improvement in the apparent SNR and an increase in the resolution of fine structure in the reconstructed image.

METHODS

Three-dimensional proton magnetic resonance images of a phantom were acquired on a 1.5-T Signa system (General

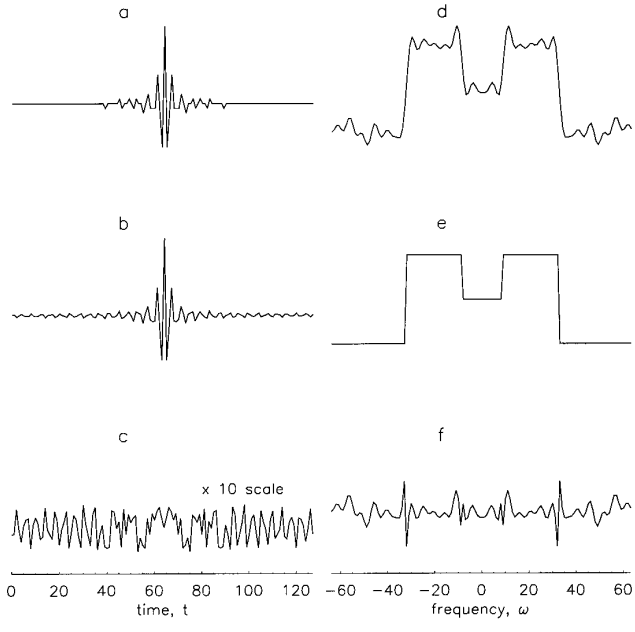

FIG. 2. Simulated one-dimensional image and its corresponding *k*-space signal. The thermal noise term, $n(t)$, was set to zero for this demonstration. The graphs correspond to the terms in Eqs. [1] and [2]. (a) The digitized *k*-space signal, $f(t)$. (b) The noise-free *k*-space signal, $s(t)$. (c) The digitization error, $d(t)$, equal to the difference of $f(t)$ and $s(t)$. (d) The image, $f(\omega)$, reconstructed from $f(t)$. (e) The noise-free image, $s(\omega)$. (f) The digitization error, $d(\omega)$, equal to the difference of $f(\omega)$ and $s(\omega)$. A 5-bit ADC was simulated to dramatize the effects of digitization. All plots are drawn to the same scale, except C, which is displayed at 10× magnification.

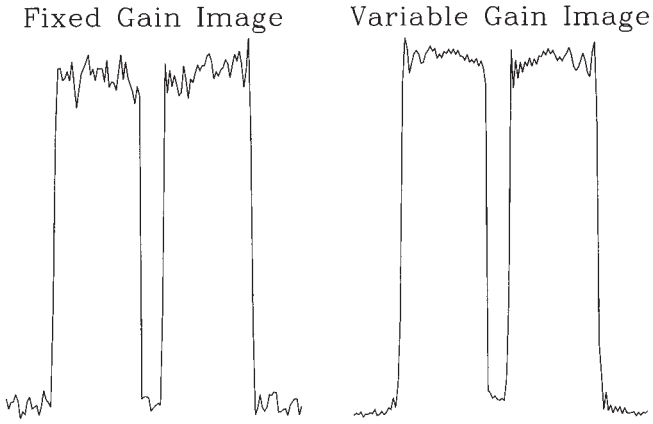

FIG. 3. Profile plots taken along an identical line in the phantom images. The region traversed by the profile plot consists of two uniformly filled water bottles separated by approximately 1 cm.

Electric Medical Systems, Milwaukee, WI). A gradient-echo sequence was used with TE = 2 ms, TR = 50 ms, a 256 × 128 × 64 encoding matrix, and a 24.0 × 24.0 × 25.6 cm FOV. The phantom was a standard head-coil phantom which contains features designed to assess image resolution. The data were acquired with a quadrature birdcage coil.

Six identical imaging sequences were repeated, each time incrementing the analog receiver gain by 6 dB. The complex *k*-space data were saved in each instance. The first data set acquired, corresponding to the lowest amount of receiver gain, was chosen such that the largest *k*-space signal filled the ADC without exceeding its maximum allowable input. Subsequent data sets were acquired with increased receiver gain, causing some of the higher amplitude phase encodings to overload the ADC. However, lower amplitude phase encodings (i.e., higher frequency rows of *k*-space) were now better digitized than their counterparts acquired at lower gain settings. After all six image data sets were acquired, the phase encodings which were digitized at the highest gain without overloading the ADC were assembled into a single 3D *k*-space data set. Each selected row of *k*-space was appropriately rescaled using high-precision (32-bit) arithmetic according to the gain level used for its acquisition. The scaling factor applied for each level of gain was determined *a priori* in calibrating the system, and consisted of both an amplitude and phase measurement. Finally, a single 3D image was constructed from the assembled *k*-space data via 3D fourier transformation. A comparison image was also constructed by transforming the *k*-space data from the lowest gain setting.

RESULTS

The image produced from the variable gain data sets shows dramatically improved SNR and resolution compared to those of the fixed gain image. Profile plots taken along identical lines in the two phantom images are shown in Fig. 3. The line traversed by the profile plots intersects two uniformly filled bottles of water separated by approximately 1 cm. The plot from the variable gain image exhibits a noticeable reduction in the noise level in both signal and signal-free regions.

Figure 4 depicts similar slices from the middle of the phantom images. Both images were indentically processed and windowed. The background noise is visibly higher in the fixed gain image. Analysis of identical signal-free regions in the two images found the root-mean-square (rms) level of the noise to be eight times smaller in the variable gain image. The rms values were computed from a region of 6400 pixels

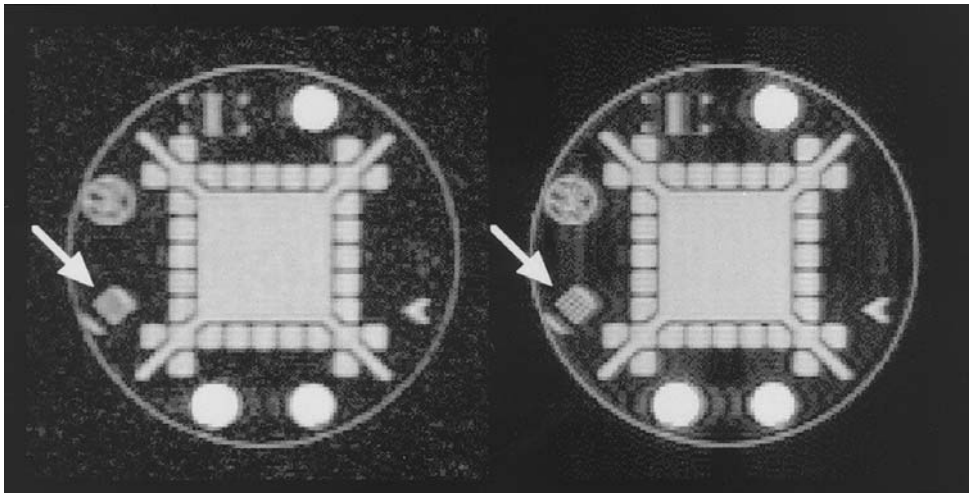

FIG. 4. Identical slices selected from the fixed (left) and variable (right) gain phantom images. Both images were identically processed and windowed. The decreased background noise level and superior resolution of the variable gain image are apparent.

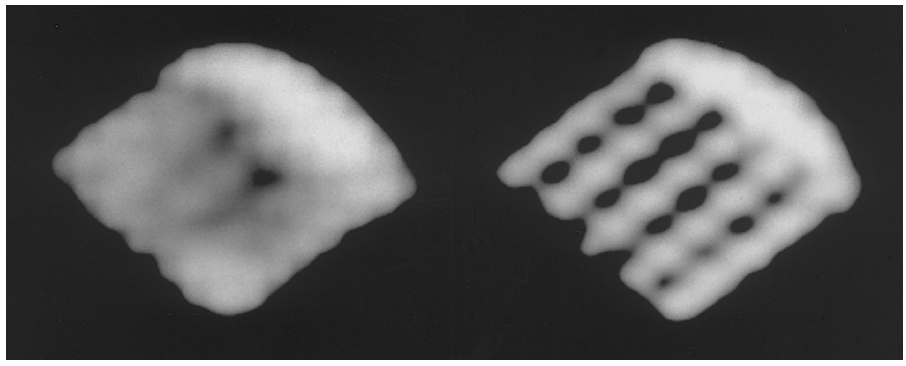

FIG. 5. Magnified region of the phantom images indicated by the arrows in Fig. 4. Images are from the fixed (left) and variable (right) gain data sets and were identically processed and windowed.

using the complex image data. The level of noise reduction was equivalent in both the real and imaginary channels.

Magnified portions of the phantom images are depicted in Fig. 5. The region, which contains a comb-shaped pattern with five teeth, has a FOV of approximately 2.7 × 2.4 cm with a nominal slice thickness of 4 mm. A comparison of the two images clearly reveals increased resolution in the image constructed from the dynamically adjusted receiver gain data sets. In the fixed gain image, the comb pattern is undetectable altogether. Figure 6 shows profile plots taken vertically through the middle of the images in Fig. 5. The profile of the variable gain image resolves the five teeth of the comb, while the fixed gain profile does not. The vertical direction of the images corresponds to a phase-encoded dimension.

DISCUSSION

The procedure outlined in this paper improves MR image quality under conditions where the image noise is dominated by digitization artifact. This is equivalent to the condition where the SNR of the largest sampled point in *k*-space exceeds the number of sampling bins of the ADC. Since the signal at the origin of *k*-space emanates from all the excited spins in the sample, large volume 3D and thick slice 2D proton images will often fall into this category. In such cases, correctly adjusting the receiver gain prior to each phase encoding can be expected to yield an increase in the SNR and resolution of the resulting image.

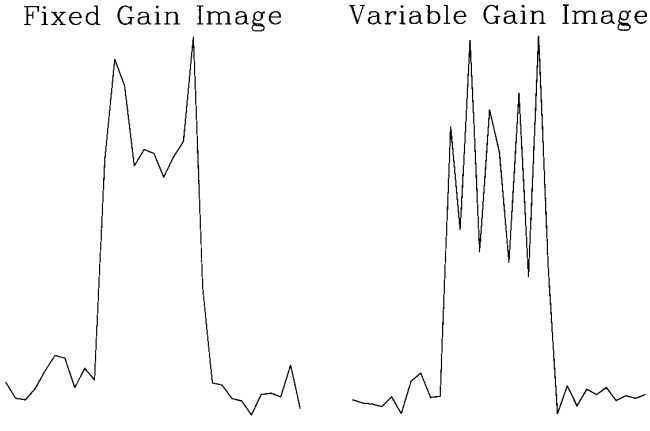

FIG. 6. Profile plots taken vertically through the middle of the images in Fig. 5. The profile of the variable gain image resolves the five teeth of the comb, while the fixed gain image does not.

The method employed in this paper required six times the experiment time needed for a single, fixed-gain image acquisition. However, this time penalty was only incurred due to software limitations of the scanner, which did not allow for changes in the analog receiver gain during imaging. Most commercial scanners available today, including the GE Signa system used in this study, vary the analog gain of the reciever by switching pin-diode attenuator circuits. Consequently, gain changes can be made in times on the order of microseconds with a simple analog or digital control line. With only a minor modification to the scanner software, the receiver gain could be adjusted prior to each phase encoding step, and no time penalty would be required to acquire an image with improved digitization.

Determining the appropriate gain levels for each phase-encoded acquisition can be accomplished by adding two additional encoding steps. Prior to the standard 3D imaging sequence, one frequency-encoded acquisition along each of the two phase-encoded axes yields an envelope of the *k*-space signal expected in the impending phase encodings. Due to the sinc-like shape of these echoes, their magnitude will not correspond directly to the maximum amplitude to be expected in each phase encoding. However, the general envelope of each echo provides a sufficient estimate of the gain needed to digitize each phase-encoded row of *k*-space without overloading the ADC. The two additional acquisitions would increase the total experiment time by only two TR periods. For the imaging protocol of 256 × 64 phase-encoding steps employed in this study, the extra acquisitions

would result in an increase in the experiment duration by just 0.01%.

Adjusting the receiver gain prior to each phase-encoded acquisition is the simplest means of increasing the dynamic range of the digitizer. However, this yields little or no enhancement in the digitization of some frequency-encoded acquisitions. A superior procedure would adjust the analog signal amplitude during the readout period as well. This would equally enhance the resolution in all three spatial dimensions, and potentially increase the overall SNR of the image even further. However, the ultimate increase in SNR is limited to the intrinsic SNR of the analog signal entering the ADC, regardless of the strategy employed. Moreover, changing the receiver gain between frequency-encoded sample points would require much faster attenuator or amplifier switching times.

It is important to note that the additional precision gained by this method essentially arises from the precision with which the various receiver gain settings are known. The rescaling step prior to image reconstruction requires that the gain levels are well calibrated. Incorrect calibration results in uneven weighting of *k*-space, possibly with adverse effects. In particular, miscalibration of the phase shift incurred by each gain level will cause ghosting artifacts which can obscure any resolution enhancement one hoped to gain.

ACKNOWLEDGMENT

This work was supported by NIH Grant RR-02305.

REFERENCES

1. A. A. Maudsley, Dynamic range improvement in NMR imaging using phase scrambling, *J. Magn. Reson.* **76,** 287–305 (1987).
2. V. J. Wedeen, Y. Chao, and J. L. Ackerman, Dynamic range compression in MRI by means of nonlinear gradient pulse, *Magn. Reson. Med.* **6,** 287–295 (1988).
3. C. H. Oh, S. K. Hilal, E. X. Wu, and Z. H. Cho, Phase-scrambled RF excitation for 3D volume-selective multislice NMR imaging, *Magn. Reson. Med.* **28,** 290–299 (1992).
4. G. Johnson, E. X. Wu, and S. K. Hilal, Optimized phase scrambling for RF phase encoding, *J. Magn. Reson. B* **103,** 59–63 (1994).
5. A. A. Maudsley, Sensitivity in fourier imaging, *J. Magn. Reson.* **68,** 363–366 (1986).
6. K. Kose, K. Endoh, and T. Inouye, Nonlinear amplitude compression in magnetic resonance imaging: Quantization noise reduction and data memory saving, *IEEE AES Magn.* **6,** 27–30 (1990).
7. J. Jackson, A. Macovski, and D. Nishimura, Low-frequency restoration, *Magn. Reson. Med.* **11,** 248–257 (1989).
8. J. C. Lindon and A. G. Ferrge, Digitisation and data processing in fourier transform NMR, *Prog. NMR Spectrosc.* **14,** 27–66 (1980).